



Article

# Discrete One-Stage Mechanochemical Synthesis of Titanium-Nitride in a High-Energy Mill

Oleg Lapshin, Olga Shkoda , Oksana Ivanova \*  and Sergey Zelepugin

Tomsk Scientific Center of the Siberian Branch of the Russian Academy of Sciences, 10/4 Akademicheskii Pr., 634055 Tomsk, Russia; ovlap@mail.ru (O.L.); o.shkoda@dsm.tsc.ru (O.S.); szel@dsm.tsc.ru (S.Z.)

\* Correspondence: bliz3@yandex.ru

**Abstract:** Discrete (discontinuous) mechanochemical synthesis of titanium nitride was experimentally investigated. The experimental results show that mechanical activation intensifies the chemical conversion in the Ti-N system, and the discrete synthesis of the final product is conducted under “soft” controlled conditions without high heat release. The new theory of mechanochemical synthesis and the mathematical model based on it were used for theoretical evaluation of the dynamics of titanium activation in the nitrogen medium. It was found that the discrete mode of synthesis includes two factors accelerating mechanochemical reactions in the Ti-N synthesis: structural (grinding of metallic reagent and formation of interfacial areas) and kinetic (accumulation of excess energy stored in the formed structural defects in metallic reagent). The kinetic constants of the process were found using experimental data and the inverse problem method. The diagrams defining the controlled modes of obtaining titanium nitride particles with the given characteristics were constructed. A mathematical model for theoretical estimation of the dynamics of activation of titanium powder in the nitrogen medium was developed using a new macrokinetic theory of mechanochemical synthesis.



**Citation:** Lapshin, O.; Shkoda, O.; Ivanova, O.; Zelepugin, S. Discrete One-Stage Mechanochemical Synthesis of Titanium-Nitride in a High-Energy Mill. *Metals* **2021**, *11*, 1743. <https://doi.org/10.3390/met11111743>

Academic Editor: Joan-Josep Suñol

Received: 30 September 2021

Accepted: 28 October 2021

Published: 30 October 2021

**Publisher's Note:** MDPI stays neutral with regard to jurisdictional claims in published maps and institutional affiliations.



**Copyright:** © 2021 by the authors. Licensee MDPI, Basel, Switzerland. This article is an open access article distributed under the terms and conditions of the Creative Commons Attribution (CC BY) license (<https://creativecommons.org/licenses/by/4.0/>).

**Keywords:** high-energy mill; mechanical activation; titanium nitride; mechanochemical synthesis; experiment; mathematical model

## 1. Introduction

Mechanochemical synthesis of inorganic substances is widely used to stimulate various solid-phase reactions and is a promising method to obtain superfine powders containing significant amounts of gaseous components. Synthesis stimulated by mechanical action has been the subject of numerous studies [1–14].

In most cases, mechanochemical synthesis can be classified as one-stage and two-stage e.g., [15–23]. One-stage mechanochemical synthesis is usually conducted in a high-energy mill in which reactive particles are milled and activated. As a consequence, due to the formation of the interfacial surface and accumulation of additional (excess) energy in the system, the chemical transformation of starting reagents into the reaction product significantly accelerates. In the case of two-stage mechanochemical synthesis, the first stage mainly involves the grinding and mechanical activation of powder mixtures, while the second stage (outside the mechanical activator) involves synthesis. As a rule, the synthesis of a mechanically pre-activated mixture was characterized by the high rates of chemical reactions.

In solid–gas systems, preliminary mechanical activation (MA) of a solid component or a mixture of solid components (silicon, aluminum, aluminum oxide, silicon oxide, yttrium oxide) also leads to the acceleration of chemical transformations during the synthesis of the product in the nitrogen medium [24–26].

The use of mechanochemical synthesis for obtaining various substances requires the ability to control the process. Of particular importance is the control of the temperature of the reacting system. Otherwise, undesirable phenomena may occur in the overheated

mechanically activated system due to phase transitions, melting, sintering, and agglomeration of reagents, etc. In addition, uncontrolled temperature increase during continuous operation of the mechanical activator can lead to intensive relaxation of accumulated excess energy due to annealing of structural defects during mechanical activation and normalization of structure in the components undergoing a phase transition.

The controlled mechanochemical synthesis, which can be achieved, in particular, by using the discontinuous operation of the mechanical activator, makes it possible to obtain particles under “soft” conditions, without a significant temperature effect in the mechanically activated system.

Three main factors lead to the acceleration of chemical reactions in the solid–gas system due to MA [10,27] for different operating modes of the mechanical activator (Figure 1):

1. Structural factor, which determines the grinding of substances and the formation of an interfacial area required for chemical interactions;
2. Kinetic factor, resulting in the accumulation of excess energy, which is accumulated in the formed structural defects of solid reagents and decreases the activation barrier of chemical reactions;
3. Temperature factor, caused by heating of milling bodies, chamber walls, and a grinding substance (dissipative heat release), as well as by heat release from the relaxation of structural defects and chemical reactions.

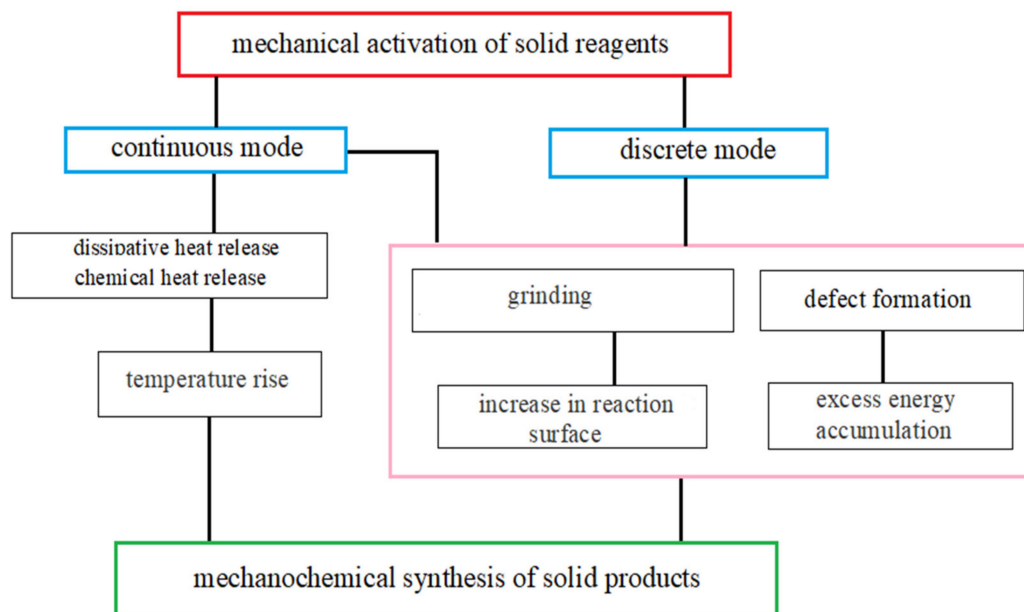


**Figure 1.** Factors accelerating chemical transformations during the synthesis of a solid-phase product (titanium nitride) when a solid reagent (titanium) is subjected to mechanical activation in a gas (nitrogen).

In [28,29], the authors determined the efficient kinetic parameters using experimental and theoretical methods and analyzed the nonisothermal chemical transformations of two-stage mechanochemical synthesis of titanium nitride. The developed mathematical model was found to be suitable for the analysis of the macrokinetics of chemical transformations in the solid reagent–active gas systems. At the same time, it can be noted that the one-stage mechanochemical synthesis in the solid–gas systems (including the Ti–N system) is still poorly studied [2,30–35].

The aim of this work is to investigate experimentally and theoretically the macrokinetics of one-stage mechanochemical synthesis in the system in the discrete (discontinuous) operating mode of the mechanical activator.

## 2. Experimental Procedure

Titanium powder (TU 14-22-57-92) was ground and mechanically activated in an M-3 planetary mill (Institute of Geology and Mineralogy, SB RAS, Novosibirsk, Russia) in nitrogen (high grade, GOST 9293-74). The initial size of titanium particles did not exceed 100  $\mu\text{m}$ . The average size of titanium particles was determined using the constructed particle size distribution histogram and was equal to 56.2  $\mu\text{m}$ . The initial nitrogen pressure in the mill drum was  $4 \times 10^5$  Pa. The volume of the steel drum was 600  $\text{cm}^3$ , and the diameter of the steel balls was 0.3–0.4 cm. The mass of the powder was 10 g, and the ball-to-powder weight ratio was 20:1. The duration of mechanical activation varied from 1 to 60 min.

The total time of MA was calculated as follows. After every 20 s of operation, the mill was stopped and the pressure of nitrogen in the drum was measured with the MT6.184 manometer. Then the temperature of the external and internal walls was measured, and the drums were cooled down in the air to room temperature. The temperature was measured with a Center 325 radiation pyrometer (Center Technology Corp., New Taipei City, Taiwan). The morphology and size of the powders were studied by scanning electron microscopy (Philips SEM515 with EDAX attachment) (Philips Belgium Commercial NV, Brussels, Belgium). The particle size diameters were measured by the SEM method. The obtained images of the powder mixture were examined with the secant method. For each MA time, at least 100 measurements were carried out. Then a histogram of particle size distribution was drawn, the average particle size was found, and the standard deviation was calculated.

The phase composition of the final products was characterized by X-ray diffraction analysis (DRON-1 and DRON-UM1,  $\text{CuK}\alpha$  radiation) (M-5912, St. Petersburg, Russia). The chemical composition of the mechanically activated powder mixture was studied by X-ray microanalysis on the CAMEBAX MICROBEAM analyzer (Gennevilliers Cedex, Gennevilliers, France) with local analysis per 1  $\mu\text{m}^3$ . The quantification accuracy was  $\pm 1.0\%$ . Transmission electron microscope studies were performed on a 125 K PEM.

## 3. Mathematical Model

For the mathematical description of the process, we used the results of a mathematical model of one-stage mechanochemical synthesis in the solid reagent–active gas system [36]. In the general case, the system of equations describing mechanochemical synthesis during mechanical activation of solid reagents in the active gas should comprise the equations of thermal balance, chemical reactions, grinding, and excess energy dynamics.

### 3.1. Thermal Balance Equation

We assume that the thermal relaxation time for milling bodies and mill walls is less than the characteristic times of chemical and dissipative heat release. In this case, there is no temperature distribution in the milling bodies and mill walls, and the thermal balance of the system is described by the following Equation (1):

$$\left(\sum_i v_i c_i \rho_i\right) \frac{dT}{dt} = v_{\Sigma} \rho_{\Sigma} \frac{d\alpha}{dt} - \frac{d}{dt}(v_{\Sigma} \Phi) + \omega - \chi \frac{S}{V} (T - T_0) \quad (1)$$

$v_i$ ,  $c_i$ ,  $\rho_i$  are the volume fraction, heat capacity, and density of the starting powder mixture ( $\Sigma$ ), gas (g), milling bodies (m), and chamber walls (s);  $t$  is the time;  $T$  is the temperature;  $\alpha$  is the chemical transformation depth defined by the ratio between the mass of the product and the total mass of the reaction system;  $Q$  is the thermal effect of reaction during the product formation;  $\Phi$  is the excess energy stored due to activation, which is proportional to the number of structural defects in the solid phase (its relaxation due to annealing or normalization of the structure due to chemical transformations will lead to excess heat release in the system);  $\omega = a_m W$  is the rate of heat release during the operation of the mill (linearly depending on the mill power  $W$ );  $a_m$  is the factor;  $\chi$  is the heat transfer coefficient

of the mill chamber with the environment;  $T_0$  is ambient temperature;  $V, S$  are the volume and surface area of the mill chamber.

In (1), the heat capacity of the powder mixture as well as the density, the volume fractions of the powder mixture and the gas can be determined by the following relations:

$$\begin{aligned} c_{\Sigma} &= c_{Ti}(1 - \alpha) + c_{TiN}\alpha, \quad \rho_{\Sigma} = \frac{\rho_{Ti}\rho_{TiN}}{\alpha\rho_{Ti} + (1-\alpha)\rho_{TiN}}, \\ \rho_g &= \frac{(1-v_{\Sigma,0})\rho_{g,0} - v_{\Sigma,0}\rho_{Ti}\alpha\mu/(1-\alpha\mu)}{1-v_{\Sigma}}, \quad v_{\Sigma} = \frac{v_{\Sigma,0}[\alpha\rho_{Ti} + (1-\alpha)\rho_{TiN}]}{\rho_{TiN}(1-\alpha\mu)}, \\ v_g &= \frac{(1-v_{\Sigma,0})\rho_{g,0} + v_{\Sigma,0}\rho_{Ti} - v_{\Sigma}\rho}{\rho_g}, \end{aligned} \quad (2)$$

$c_{Ti}, c_{TiN}, \rho_{Ti}, \rho_{Ti}, \rho_{TiN}$  are the heat capacity and density of titanium and titanium nitride;  $v_{\Sigma,0}$  is the initial volume fraction of the powder mixture;  $\mu$  is the mass fraction of gas in the product (titanium nitride).

### 3.2. Chemical Transformation Equation

The rate of irreversible reaction between the activated solid reagent and gas is written as

$$\frac{d\alpha}{dt} = K(T)f(\alpha)F(S) \left( \frac{p}{p_0} \right)^n \quad (3)$$

$K(T) = k_0 \exp(-E/RT)$  is the constant of the reaction rate;  $k_0$  is pre-exponent;  $E$  is the effective activation energy of chemical reactions;  $R$  is the universal gas constant;  $p_0, p$  are the normal and current gas pressure;  $n$  is exponent;  $f(\alpha)$  is the kinetic reaction law.

The effect of excess energy accumulated in the structural defects of the solid reagent (titanium) on the effective activation energy of the chemical reaction is expressed as follows:

$$E = E_0 - \varphi_{Ti} \quad (4)$$

$E_0$  is the activation energy of the chemical reaction in the absence of mechanical treatment;  $\varphi_{Ti}$  is the amount of accumulated excess energy in the reagent (titanium).

The pressure in (2) is related to the current density of the gas  $\rho_g$  by the equation of state:

$$p = \frac{\rho_g}{M_g} RT \quad (5)$$

$M_g$  is the molecular mass of the gas.

In (4), the dimensionless function characterizing the change of reaction surface  $F(S)$  is defined as the ratio of the current particle surface area  $S$  to its initial value  $s_0$ :

$$F(S) = \frac{S}{s_0} \quad (6)$$

$s_0 = N_0 4\pi r_0^2, s = N 4\pi r^2; N_0, N$  are initial and current number of particles in the system;  $r_0, r$  are the initial and current particle sizes.

### 3.3. Grinding Equation

Particle size depends on the rate of particle size reduction and volumetric changes during chemical transformations. The dynamics of the change in the specific surface of particles during chemical transformations and grinding can be written in the form:

$$\frac{dr}{dt} = \frac{\partial r}{\partial \varepsilon} \frac{d\varepsilon}{dt} + \frac{\partial r}{\partial \alpha} \frac{d\alpha}{dt} \quad (7)$$

$\varepsilon = kW/V_{\Sigma}t$  is the energy per unit volume of the ground body;  $V_{\Sigma} = v_{\Sigma}V_k$ —is the volume of condensed phase;  $V_k$  is the volume of the mill chamber;  $k$  is the coefficient determining the mill's grinding capacity. The first term in Equation (5) describes the dynamics of the specific surface of particles due to grinding in the absence of chemical

reactions, and the second term due to chemical reactions in the absence of grinding. In [36], it is believed that in the case of fine grinding a lot of energy is spent on inelastic deformation, the work of friction forces, and the formation of new surfaces. In this case, the derivatives included in (7) in [36] can be represented as follows:

$$\frac{\partial r}{\partial \varepsilon} = \frac{r(r_m - r)}{3A}, \quad \frac{\partial r}{\partial \alpha} = -\frac{r(1 - \mu)}{3(1 - \alpha\mu)(1 - \alpha)},$$

$r_m$  is the minimum particle size achieved in the grinding process;  $A$  is a coefficient.

### 3.4. Dynamics of Excess Energy

Two parallel processes take place during mechanical treatment: structural imperfections (and accumulation of excess energy) and their relaxation (reduction of excess energy). Structural imperfections during MA are very diverse, which makes it difficult to choose the kinetics of structure normalization. We will assume that the dynamics of excess energy in titanium and titanium nitride can be described by the following kinetic equations [36]:

$$\frac{d\phi_{Ti}}{dt} = a_{Ti} \frac{W}{V_{\Sigma}} - \phi_{Ti} n_{Ti} \exp\left(-\frac{U_{Ti} - \phi_{Ti}}{RT}\right) \quad (8)$$

$$\frac{d\phi_{TiN}}{dt} = a_{TiN} \frac{W}{V_{\Sigma}} - \phi_{TiN} n_{TiN} \exp\left(-\frac{U_{TiN} - \phi_{TiN}}{RT}\right) - \frac{\phi_{TiN}}{\alpha(1 + b\alpha)} \frac{d\alpha}{dt} \quad (9)$$

In (8) and (9), the first term determines the rate of accumulation of excess energy, the second term determines the rate of relaxation of excess energy, and the third term in (9) determines the rate of normalization of the solid phase structure due to chemical transformation.

In (8) and (9), the following notations are introduced:  $n_{Ti}$ ,  $n_{TiN}$  are pre-exponential multipliers;  $U_{Ti}$ ,  $U_{TiN}$  are the activation energies of relaxation of the excess energy in titanium and titanium nitride;  $\phi_{Ti}$ ,  $\phi_{TiN}$  are the specific excess energy in titanium and product;  $a_{Ti}$ ,  $a_{TiN}$  are the coefficients determining the mill capacity for the formation of structural defects in titanium and a reaction product;  $b = (\rho_{Ti} - \rho_{TiN}) / \rho_{TiN}$ ;  $\rho_{Ti}$ ,  $\rho_{TiN}$  are the titanium and titanium nitride densities.

The ratio for the total specific excess energy in the condensed phase:

$$\phi = (1 - \alpha)v_{\Sigma}\phi_{Ti} + \alpha v_{\Sigma}\phi_{TiN} \quad (10)$$

Initial conditions.

$$t = 0: T = T_0, r = r_0, p = p_0, \alpha = 0, \phi_{Ti} = \phi_{TiN} = 0. \quad (11)$$

For the case of discontinuous mechanosynthesis, we can write:

$$W = \begin{cases} > 0, t - (j - 1)(\tau_a + \tau_0) < \tau_a \\ 0, t - (j - 1)(\tau_a + \tau_0) \geq \tau_0 \end{cases} \quad (12)$$

$j$  is the current number of the mill switches ( $j=1 \dots N$ );  $N$  is the number of cycles;  $\tau_a$  is the duration of the mill operation for one cycle (the time between two adjacent mill switches is taken as a one cycle);  $\tau_0$  is the duration of the mill stop in one cycle;  $t_a = N\tau_a$  is the mechanical activation time;  $t_m = (N - 1)(\tau_a + \tau_0) + \tau_a$  is the total mechanical treatment time.

Let us make some assumptions. We assume that the kinetic function obeys the parabolic law  $f(\alpha) = 1/\alpha$ , and the exponent  $n = 1$ . We will also neglect the relaxation rate of structural defects due to annealing compared to the rate of their accumulation. In addition, we consider that  $a_{Ti} = a_{TiN} \approx a$ .

#### 4. Solution of the Problem and Discussion

To solve this problem, the following initial data were used [29,37]:  $c_{Ti} = 528 \text{ J}/(\text{kgK})$ ,  $c_s = c_m = 462 \text{ J}/(\text{kgK})$ ,  $\rho_{Ti} = 4500 \text{ kg}/\text{m}^3$ ,  $\rho_s = \rho_m = 7900 \text{ kg}/\text{m}^3$ ,  $Q = 5.8 \times 10^5$ ,  $E = 141,510 \text{ J}/\text{mol}$ ,  $k_0 = 2.8 \times 10^4 \text{ s}^{-1}$ ,  $M_g = 28 \times 10^{-3} \text{ kg}/\text{mol}$ ,  $\mu = 0.23$ ,  $b = -0.17$ ,  $\omega / \sum(v_i c_i \rho_i) = 70 \text{ K}/\text{min}$ ,  $V = 6 \times 10^{-2} \text{ m}^3$ ,  $S = 0.72 \text{ m}^2$ . It was assumed that for the running mill the coefficient  $\chi = 10 \text{ J}/(\text{s K m}^2)$ , and for the stop of the mill under forced cooling conditions  $\chi = 1000 \text{ J}/(\text{s K m}^2)$ .

##### 4.1. Estimation of Kinetic Parameters

Figure 2 shows the average size of titanium particles (a), the temperature on the internal ( $T_{in}$ ) and external ( $T_{on}$ ) surfaces of the drum wall (b), as well as the nitrogen pressure in the mill chamber (c) as a function of the MA time. It can be seen that the size of titanium particles decreases to  $28 \mu\text{m}$ , and then, during the agglomeration of particles, it increases and becomes  $48 \mu\text{m}$  after 5 min MA. With increasing the MA time, the titanium particles are ground again and their size achieves 20 microns for 10–20 min. The temperature on the chamber wall due to the discrete operation of the mill and its cooling during the stop changes insignificantly and is approximately equal to its initial value. The nitrogen pressure in the chamber up to 19 min MA also remains constant. At 20 min MA, there is a sharp decrease in nitrogen pressure, indicating the start of an intense chemical reaction with gas absorption during the synthesis of titanium nitride. At this moment, a slight temperature jump (up to  $10 \text{ }^\circ\text{C}$ ) occurs on the surface of the mill wall due to the heat released during the formation of the final product. A similar temperature jump (less than  $10 \text{ }^\circ\text{C}$ ) during mechanosynthesis of titanium nitride in a high-energy mill was recorded by the authors of [34]. The authors denoted this temperature jump as the peak of combustion and synthesis. We believe that a further increase in the mechanical activation time will provide a decrease in the rate of chemical conversion since nitrogen begins to react with the remaining reagent (titanium) through an intermediate barrier (formed layer of titanium nitride). Note that the XRD data presented in Figure 9, including those for the times exceeding 20 min MA, show that at 40 min MA the titanium reflexes are no longer observed (only reflexes belonging to the titanium nitride are visible).

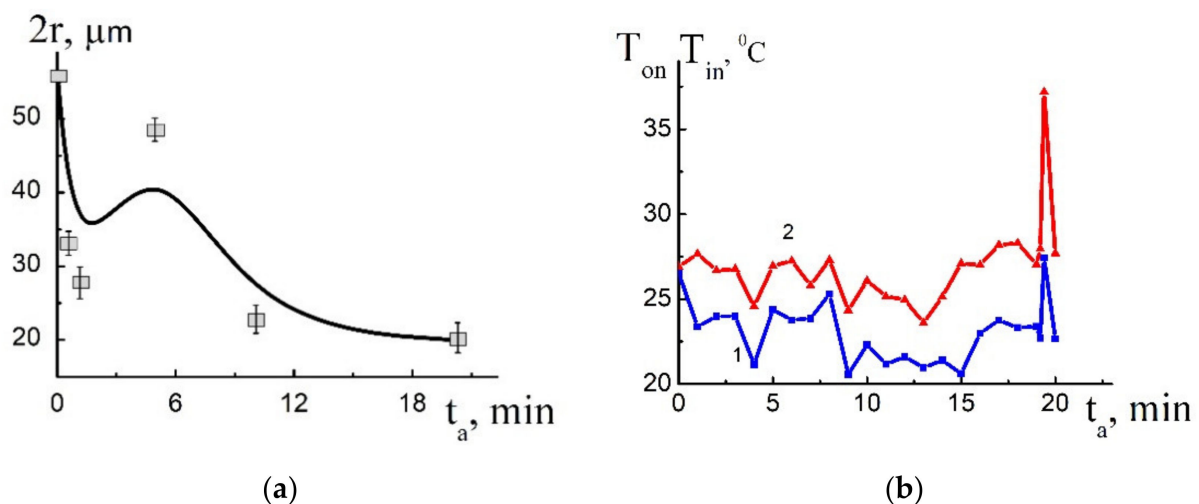
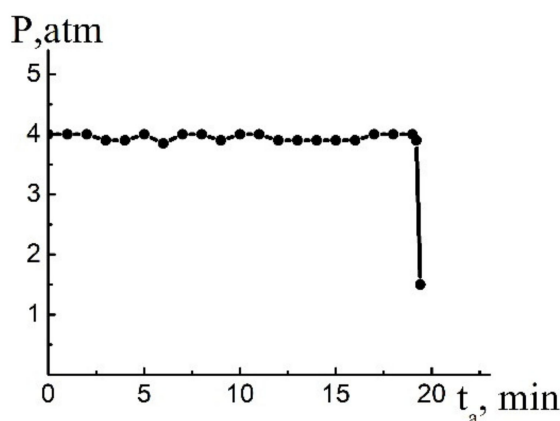


Figure 2. Cont.



(c)

**Figure 2.** (a) Experimental dependences of the size of titanium particles, (b) the temperature on the external (curve 1) and internal (curve 2) surfaces of the mill wall, (c) nitrogen pressure in the mill on the mechanical activation time  $t_a$  for  $m_{\Sigma,0} = 0.0037$ .

The experimental dependence of the titanium particle size on the MA time (Figure 2a) was used to find the grinding parameter  $K = k'W/V_k$  (where  $k' = k/(3A)$ ) included in Equation (6). For this purpose, neglecting the influence of the chemical reaction on grinding, Equation (7) is reduced to the form:

$$Y = \frac{1}{r_m} \ln \left[ \frac{r(r_m - r_0)}{r_0(r_m - r)} \right] = \frac{K}{v_{\Sigma,0}} t_a \quad (13)$$

Analyzing Figure 2a, in (13) we can take  $r_m \approx 10 \mu\text{m}$ .

The results of processing the experimental data by the least-squares method in the coordinates of the straight line Equation (13) are shown in Figure 3. The slope of the straight line to the abscissa axis determines the value  $K = 7.8 \times 10^{-5} \text{ min}^{-1}$ . From here we can find the coefficient characterizing the grinding for the given type of mill  $k' = 2 \times 10^{-13} \text{ min m}^2$ . The value of the complex  $\Omega = aW/V_k$  characterizing the rate of accumulation of excess energy in the condensed phase during MA was found by fitting the numerical calculation to the experimental data. The fitting criterion was the time of the start of intensive chemical reaction equal to 19.4 min MA. It was found that the value of  $\Omega = 18.5 \text{ J}/(\text{mol min})$ . Further, we calculated the coefficient characterizing the rate of accumulation of excess energy in the solid phase  $a = 3.84 \times 10^{-3} \text{ m}^4/\text{min}$ .

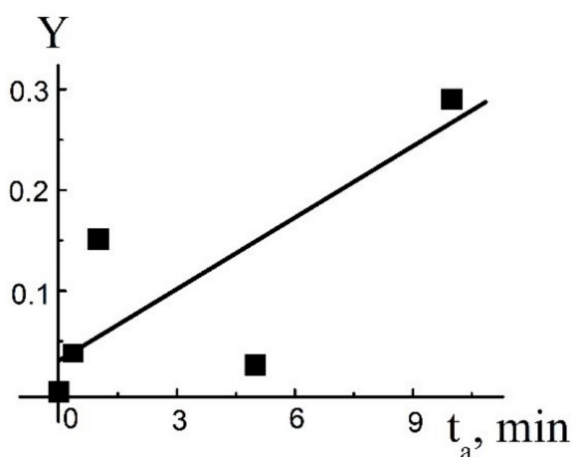


**Figure 3.** Processing of experimental data using the least-squares method for  $m_{\Sigma,0} = 0.0037$ .

The determined coefficients  $k'$  and  $a$  along with the use of the mathematical model (1)–(11) can be used to perform quantitative estimations of one-stage mechanochemical synthesis in the Ti-N system varying the following parameters: the mass of powder mixture in the mill, and the capacity and volume of the mill chamber.

#### 4.2. Numerical Solution of the Problem

Figure 4 shows the temperature dependences for the continuous (curve 1) and discontinuous (curves 2 and 3) operation modes of the mechanical activator. At the beginning of the process, a linear temperature rise is observed due to high heat release during the operation of the mill. When the activated system reaches sufficiently high temperatures, there is a thermal explosion (temperature break in the thermogram) caused by the acceleration of the chemical reaction during the formation of titanium nitride. After completion of the reaction, there is a further linear increase in the temperature due to the operation of the mechanical activator.

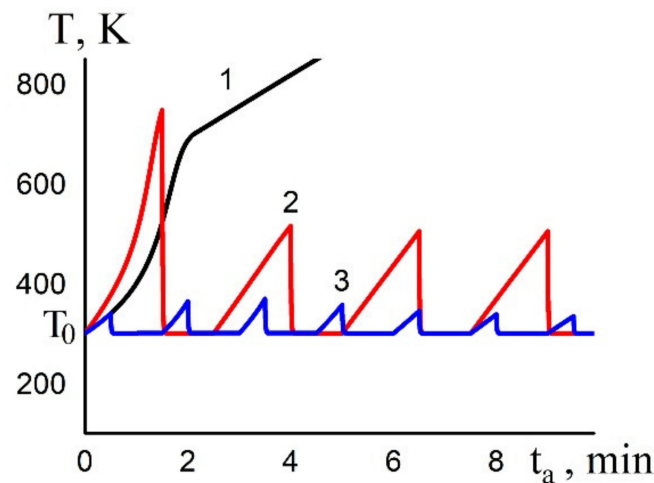


**Figure 4.** Theoretical dependences of temperature in the mechanically activated solid reagent–active gas system on the mechanical activation time for different activation modes and  $m_{\Sigma,0} = 0.37$ : 1—continuous; 2—discontinuous ( $\tau_a/\tau_0 = 1.5$ ); 3—discontinuous ( $\tau_a/\tau_0 = 0.5$ ).

For the discrete mode, with an increase in the stop of the mechanical activator in comparison with the time of its operation, the rate of the temperature rise decreases. The discrete mode of mechanochemical synthesis permits the transition from explosive modes of chemical interactions (curve 1) with rapid heating of the mill and intense chemical transformations to low-temperature mechanical activation under the controlled ignition limit (curves 2 and 3).

Next, we consider the operation of the mechanical activator in the discrete mode, when the dissipative heat release is neglected.

The numerical calculations of the mechanochemical synthesis of titanium nitride as a function of the operating time of the high-energy mill are demonstrated in Figure 5a–c. During mechanical activation, the particles of the condensed phase are ground with a decrease in their size (a). With increasing the MA duration under conditions of the gradual accumulation of excess energy in the solid component, a significant decrease in the activation energy  $E_{\text{eff}} = E - \varphi$ , which determines the chemical interaction between titanium and nitrogen (b, curve 2), is observed.



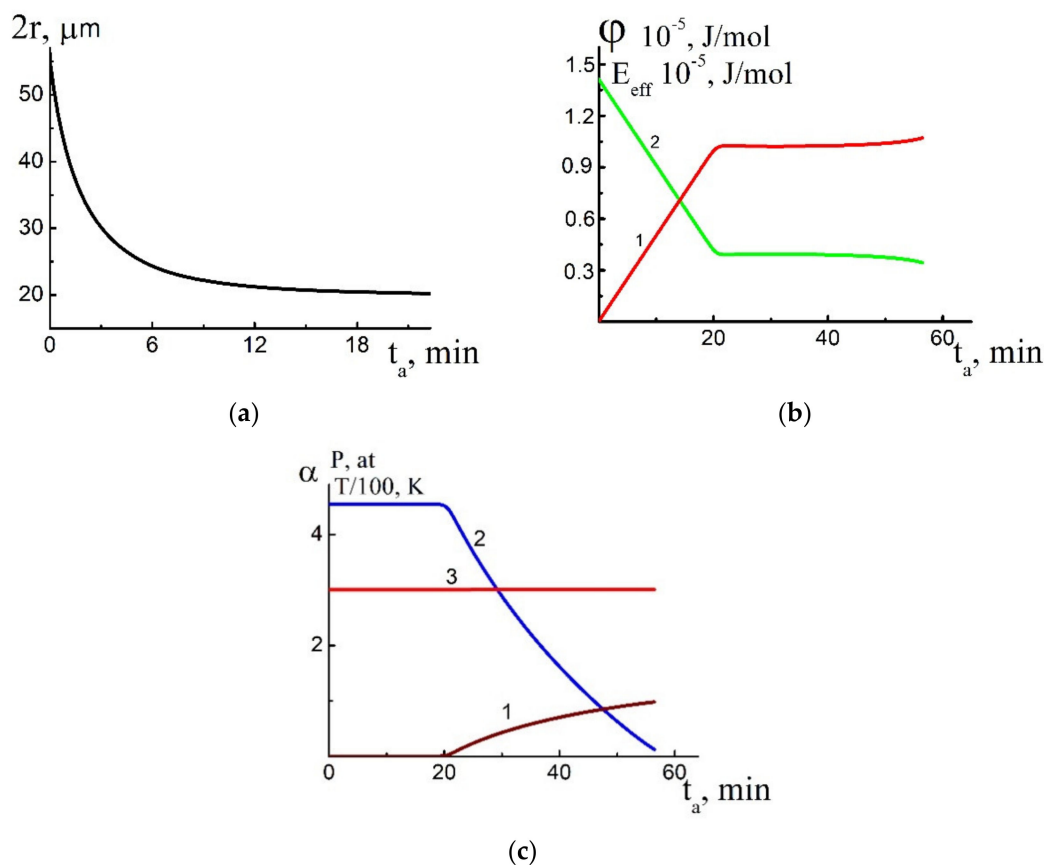


**Figure 5.** (a) Theoretical dependencies of particle size, (b) excess energy (curve 1), activation energy (curve 2), (c) depth of chemical transformations (curve 1), nitrogen pressure in the chamber (curve 2), and temperature of the system (curve 3) for grinding of titanium powder in nitrogen for  $m_{\Sigma,0} = 0.0037$ .

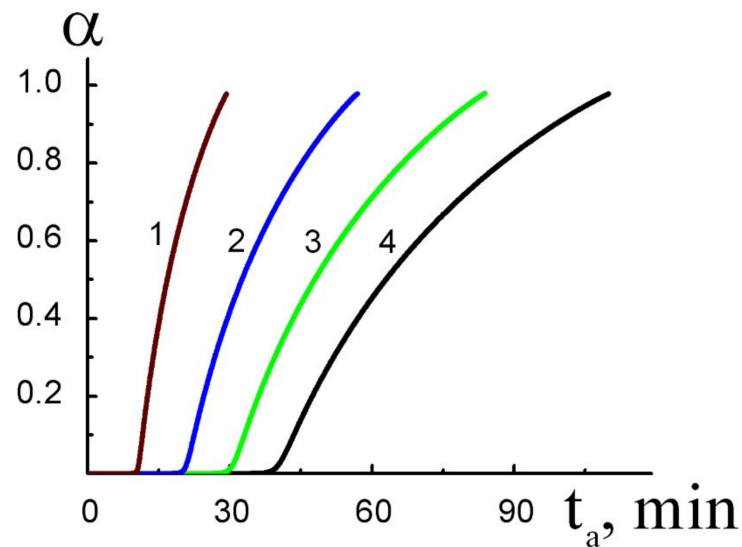
It is worth noting that the parameters  $\varphi$  and  $E_{\text{eff}}$  remain practically constant during synthesis. This fact can be explained by the achieved equilibrium between the rates of accumulation of excess energy in the condensed phase and its relaxation during chemical transformations. The calculations showed that the  $E_{\text{eff}}$  value during MA decreased by a factor of 4.3. It was noted earlier in [38] that the activation energy in some condensed systems decreased by more than 3 times relative to its initial value after the preliminary MA.

The growth of the interfacial area and the decrease in the activation energy of the product formation during MA intensifies the chemical interaction and leads to an increase in the depth of chemical transformations (5c, curve 1). Due to the nitrogen absorption by the condensed phase during the chemical reaction, the pressure of the remaining free gas in the chamber sharply decreases at the 20 min MA (5c, curve 2). The calculations show that the temperature of the system during the MA process remains unchanged (5c, line 3). The theoretical calculations presented in Figure 5 are in good agreement with the experimental data (Figure 2).

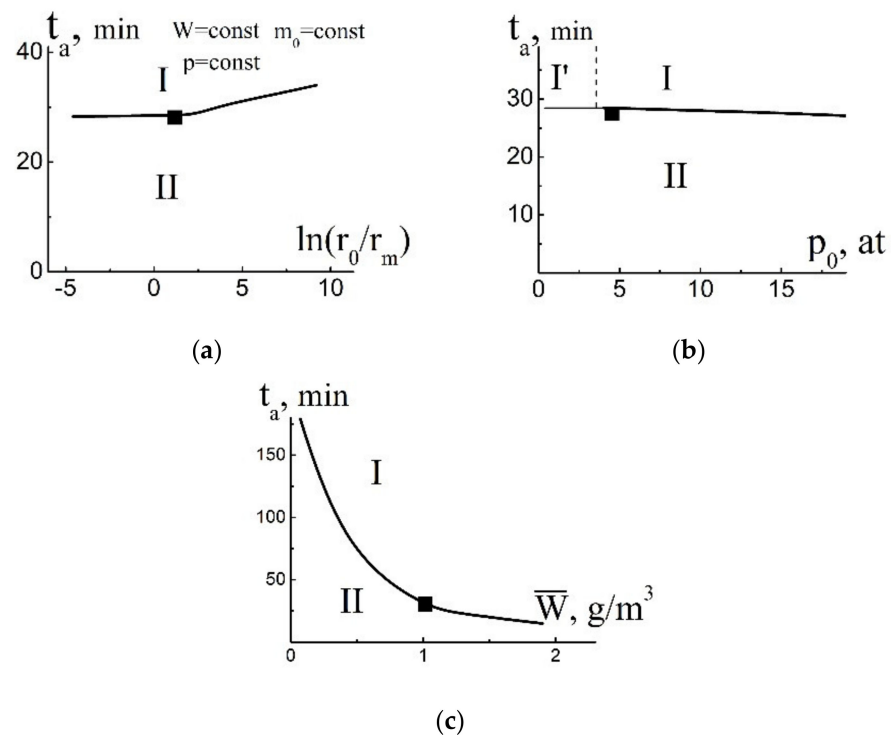
The values of  $K$  and  $\Omega$  determined above by the inverse problem method optimize the mechanochemical synthesis of titanium nitride. For example, the constructed mathematical model can be used to make a quantitative prognostic estimation of the time of transformation of reagents into a reaction product. In this case, the unproductive energy consumption for grinding and activation is reduced in the experiment.

Figure 6 shows the numerical calculations of the kinetic dependences of the chemical transformation depth in the titanium–nitrogen system on the initial volume fraction of titanium  $m_{\Sigma,0}$  in the mill. It can be seen that, with the increase of the parameter  $m_{\Sigma,0}$ , the time of the transformation of the reagents into the reaction product increases. The predictive diagrams describing the modes of one-stage mechanochemical synthesis of

titanium nitride, depending on the process-determining parameters are shown in Figure 7. The symbol ■ denotes the initial conditions of the experiments used to find the coefficients  $k'$  and  $a$ . The lines in the diagrams were obtained by calculation and divide diagrams into several regions.



**Figure 6.** Numerical calculations of the depth of chemical transformations in the mechanically activated system Ti-N for different values of the parameter  $m_{\Sigma,0}$ : 1—0.00185, 2—0.0037, 3—0.0056, 4—0.0074.



**Figure 7.** (a) Diagrams defining the different modes of mechanical activation of titanium powder in nitrogen depending on the initial size of titanium particles  $r_0$ , (b) initial nitrogen pressure, (c) specific power of the mill  $\bar{W} = W/V_{\Sigma,0}$ .

Region I defines the modes of mechanochemical synthesis corresponding to the complete transformation of the starting reagents into the final product. Here  $t_a \geq t_*$ ,  $\alpha \approx 1$ , the degree of the product activation can be estimated by the approximate formula:

$$\phi_{\text{TiN}} \approx a \frac{W}{V_{\Sigma,0}} (t - t_*) \quad (14)$$

In (14), the value  $t_*$  is the minimum mechanical activation time required to implement mechanochemical synthesis. The parameter  $t_*$  can be estimated by the analytical formula obtained from the solution of system (1)–(9):

$$t_* \approx A \frac{V_{\Sigma,0}}{W} \ln \left( 1 + \frac{BWr_0}{V_{\Sigma,0}p_0^n} \right) \quad (15)$$

$$A = RT/a, B = RTr_m p_*^n / [aK(T)].$$

Region II contains the modes with insufficient mechanical activation time for the synthesis of titanium nitride. In this case  $t_a < t_*$ ,  $\alpha \approx 0$ , and the activation degree of titanium powder in the high-energy mill can be found from the following relation:

$$\phi_{\text{Ti}} \approx a \frac{W}{V_{\Sigma,0}} t \quad (16)$$

Region I' corresponds to the modes of mechanosynthesis with incomplete transformation of titanium powder due to the lack of nitrogen gas in the mill chamber. In this case  $t_a \geq t_*$ , the depth of chemical transformation  $\alpha < 1$ , and its final value can be determined by the formula:

$$\alpha = \frac{(1 - v_{\Sigma,0})\rho_{g,0}}{\mu[(1 - v_{\Sigma,0})\rho_{g,0} + v_{\Sigma,0}\rho_{\text{Ti}}]} \quad (17)$$

The activation degree of the product and unspent titanium in Region I' can be estimated from relations (15) and (16).

#### 4.3. Morphology and X-ray Diffraction of the Final Product

The morphology of the powder mixture and X-ray diffraction patterns of the synthesized product as a function of the MA time are shown in Figures 8 and 9.

Starting titanium powder consists of plate-like-coral shaped particles (Figure 8a). During MA up to 1 min, the particles are crushed into irregularly shaped fragments. Increasing the MA time to 10 min insignificantly affects the shape of powder titanium particles. The particles remain plate-shaped with an average size of about 50  $\mu\text{m}$  (b). A further increase in the mechanical activation time (up to 50 min) changes the morphology of the product particles. They acquire a round shape with a diameter of about 1  $\mu\text{m}$ . For this period of MA, the plate-shaped particles in the mixture are not detected (c).

The X-ray diffraction pattern of the reaction product shows almost the complete interaction of activated titanium powder with nitrogen for 50 min MA (Figure 9). With increase of the mechanical activation time, the fraction of stoichiometric titanium nitride in the powder mixture also increases. These data are in good agreement with the theoretical calculations (curve 2 in Figure 6) corresponding to the experimental conditions ( $m_{\Sigma,0} = 0.0037$ ).

The final products of the mechanical nonisothermal synthesis are agglomerates consisting of spherical and rounded particles of near stoichiometric titanium nitride with a size ranging from 100 to 300 nm. The content of nitrogen in titanium nitride is shown in Figure 10.

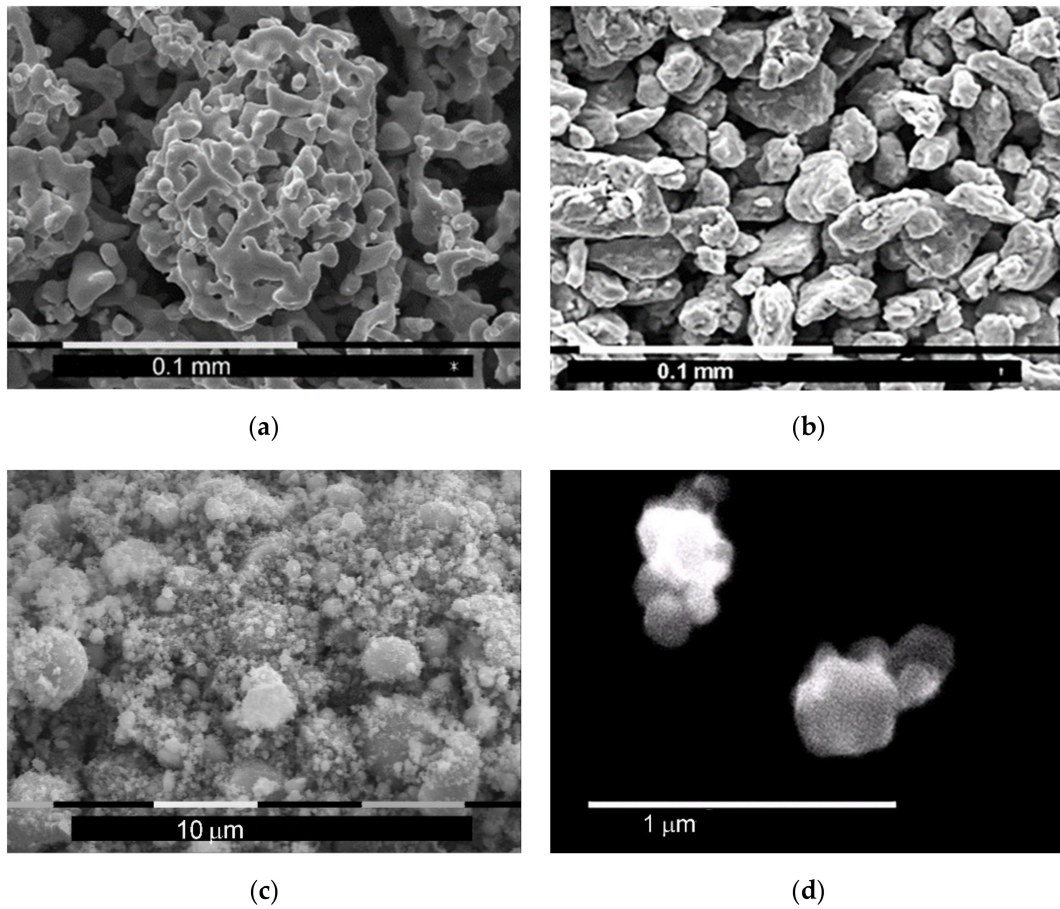


**Figure 8.** Morphology of titanium powder as a function of the MA time, min: (a) 0, (b) 10, (c) 40, (d) microphotograph of titanium nitride particles obtained by mechanochemical synthesis, data from [29].

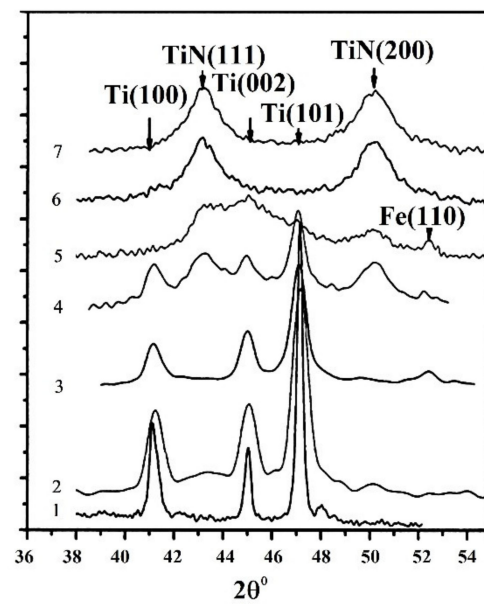


**Figure 9.** X-ray diffraction patterns depending on the duration of mechanical activation in a high-energy mill: 1—0 min, 2—5 min, 3—10 min, 4—20 min, 5—30 min, 6—40 min, 7—50 min.

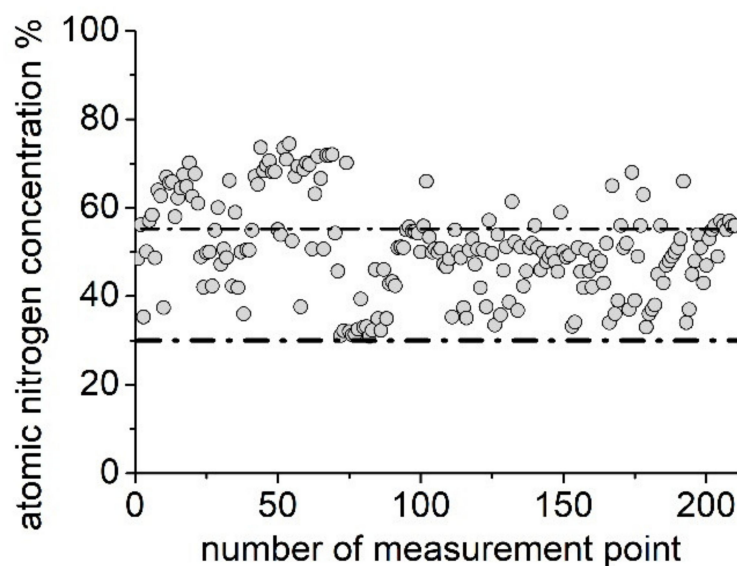


**Figure 10.** Content of nitrogen in titanium nitride according to XRD micro-analysis of mechanically activated titanium powder in nitrogen after 20 min MA.

It should be noted that the microanalysis did not show pure titanium, although the XRD shows its lines. This can be explained by the fact that the penetration depth of X-rays in the XRD analysis and XRD microanalysis is different. Microanalysis can be used at a smaller depth and this means that the surfaces of the titanium particles have interacted with nitrogen to some extent. The homogeneous area of titanium nitride ranges from 30 at% to 55 at% nitrogen [39]. The crystal lattice parameter is 4.221 Å, which corresponds to the literature data [39].

## 5. Conclusions

A macroscopic mathematical model of one-stage discrete mechanochemical synthesis of titanium nitride in the high-energy mill was developed using experimental data.

Mechanical activation was found to intensify chemical transformations in the system Ti-N. The discrete operation of the mechanical activator makes it possible to synthesize a final product under “soft” conditions without high heat release. It was established that the discrete operating mode of the mechanical activator includes two factors accelerating mechanochemical reactions during the synthesis of TiN: structural (grinding of solid particles and formation of interfacial areas) and kinetic (accumulation of excess energy stored in the formed structural defects).

The kinetic constants of the grinding and activation of titanium powder particles in the nitrogen medium were determined using experimental data and the constructed mathematical model.

Approximate analytical relations and prognostic diagrams were obtained to determine different modes of one-stage mechanochemical synthesis of titanium nitride. The diagrams also can be used to optimize this process.

**Author Contributions:** Conceptualization, O.L.; methodology, O.L. and O.S.; formal analysis, O.L. and S.Z.; investigation, O.L. and O.S.; data curation, O.L., O.I. and S.Z.; Writing—Original draft preparation, O.L. and O.S.; Writing—Review and editing, O.I. and S.Z.; visualization, O.L. and O.S. All authors have read and agreed to the published version of the manuscript.

**Funding:** The study was not supported by any grant.

**Data Availability Statement:** All data included in this study are available upon request by contact with the corresponding author.

**Conflicts of Interest:** The authors declare no conflict of interest.

## References

1. Takacs, L. The historical development of mechanochemistry. *Chem. Soc. Rev.* **2013**, *42*, 7649–7659. [[CrossRef](#)]
2. Rogachev, A.S. Mechanical activation of heterogeneous exothermic reactions in powder mixtures. *Russ. Chem. Rev.* **2019**, *88*, 875–900. [[CrossRef](#)]
3. Andreev, D.; Vdovin, Y.; Yuhvid, V.; Golosova, O. Mo–Nb–Si–B Alloy: Synthesis, Composition, and Structure. *Metals* **2021**, *11*, 803. [[CrossRef](#)]
4. Yeh, C.-L.; Chen, K.-T. Synthesis of FeSi–Al<sub>2</sub>O<sub>3</sub> Composites by Autowave Combustion with Metallothermic Reduction. *Metals* **2021**, *11*, 258. [[CrossRef](#)]
5. Dome, K.; Podgorbunskikh, E.; Bychkov, A.; Lomovsky, O. Changes in the Crystallinity Degree of Starch Having Different Types of Crystal Structure after Mechanical Pretreatment. *Polymers* **2020**, *12*, 641. [[CrossRef](#)] [[PubMed](#)]
6. Loubes, M.A.; González, L.C.; Tolaba, M.P. Modeling energy requirements in planetary ball milling of rice grain. *Part. Sci. Technol.* **2021**. [[CrossRef](#)]
7. García-Garrido, C.; Ferrer, R.S.; Salvo, C.; García-Domínguez, L.; Pérez-Pozo, L.; Lloreda-Jurado, P.; Chicardi, E. Effect of Milling Parameters on the Development of a Nanostructured FCC–TiNb15Mn Alloy via High-Energy Ball Milling. *Metals* **2021**, *11*, 1225. [[CrossRef](#)]
8. Hirosawa, F.; Iwasaki, T. Dependence of the dissipated energy of particles on the sizes and numbers of particles and balls in a planetary ball mill. *Chem. Eng. Res. Des.* **2021**, *167*, 84–95. [[CrossRef](#)]
9. Bernauer, C.; Grohmann, S.; Angermann, P.; Dickes, D.; Holzberger, F.; Amend, P.; Zaeh, M. Investigation of the Cause-Effect Relationships between the Exothermic Reaction and the Microstructures of Reactive Ni–Al Particles Produced by High Energy Planetary Ball Milling. *Metals* **2021**, *11*, 876. [[CrossRef](#)]
10. Lapshin, O.V.; Boldyreva, E.V.; Boldyrev, V.V. Role of Mixing and Milling in Mechanochemical Synthesis (Review). *Russ. J. Inorg. Chem.* **2021**, *66*, 433–453. [[CrossRef](#)]
11. Michalchuk, A.A.L.; Boldyreva, E.V.; Belenguer, A.M.; Emmerling, F.; Boldyrev, V.V. Tribochemistry, Mechanical Alloying, Mechanochemistry: What is in a Name? *Front. Chem.* **2021**, *9*, 685789. [[CrossRef](#)] [[PubMed](#)]
12. Kochetov, N.; Sytshev, A. Effects of magnesium on initial temperature and mechanical activation on combustion synthesis in Ti–Al–Mg system. *Mater. Chem. Phys.* **2021**, *257*, 123727. [[CrossRef](#)]
13. Shuck, C.E.; Manukyan, K.V.; Rouvimov, S.; Rogachev, A.S.; Mukasyan, A.S. Solid-flame: Experimental validation. *Combust. Flame* **2016**, *163*, 487–493. [[CrossRef](#)]
14. Delogu, F.; Takacs, L. Mechanochemistry of Ti–C powder mixtures. *Acta Mater.* **2014**, *80*, 435–444. [[CrossRef](#)]
15. Shkoda, O.A.; Lapshin, O.V. Thermal Explosion in a Mechanically Activated Ti–Ni System. Experimental Data. *Russ. Phys. J.* **2016**, *59*, 1231–1234. [[CrossRef](#)]
16. Lapshin, O.V.; Shkoda, O.A. Thermal Explosion in a Mechanically Activated Ti–Ni System: Mathematical Model. *Russ. Phys. J.* **2017**, *59*, 1433–1439. [[CrossRef](#)]
17. Shkoda, O.A.; Lapshin, O.V. Mechanical Activation and Thermal Treatment of Low-Energy Nb–2Si Powder Blend. I. the Experiment. *Russ. Phys. J.* **2019**, *61*, 1951–1955. [[CrossRef](#)]
18. Lapshin, O.V.; Shkoda, O.A. Mechanical Activation and Thermal Treatment of Low-Energy Nb–2Si Powder Blend. The Experiment. II. Mathematical Model. *Russ. Phys. J.* **2019**, *61*, 2209–2217. [[CrossRef](#)]
19. White, J.D.E.; Reeves, R.V.; Son, S.F.; Mukasyan, A.S. Thermal Explosion in Al–Ni System: Influence of Mechanical Activation. *J. Phys. Chem. A* **2009**, *113*, 13541–13547. [[CrossRef](#)]
20. Shteinberg, A.S.; Lin, Y.-C.; Son, S.; Mukasyan, A. Kinetics of High Temperature Reaction in Ni–Al System: Influence of Mechanical Activation. *J. Phys. Chem. A* **2010**, *114*, 6111–6116. [[CrossRef](#)]
21. Aly, Y.; Schoenitz, M.; Dreizin, E.L. Ignition and combustion of mechanically alloyed Al–Mg powders with customized particle sizes. *Combust. Flame* **2013**, *160*, 835–842. [[CrossRef](#)]
22. Aly, Y.; Dreizin, E.L. Ignition and combustion of Al–Mg alloy powders prepared by different techniques. *Combust. Flame* **2015**, *162*, 1440–1447. [[CrossRef](#)]
23. Terry, B.; Son, S.; Groven, L.J. Altering combustion of silicon/polytetrafluoroethylene with two-step mechanical activation. *Combust. Flame* **2015**, *162*, 1350–1357. [[CrossRef](#)]
24. Jin, H.-B.; Yang, Y.; Chen, Y.-X.; Lin, Z.-M.; Li, J.-T. Mechanochemical-Activation-Assisted Combustion Synthesis of  $\alpha$ -Si<sub>3</sub>N<sub>4</sub>. *J. Am. Ceram. Soc.* **2006**, *89*, 1099–1102. [[CrossRef](#)]
25. Chen, Y.-X.; Li, J.-T.; Du, J.-S. Cost effective combustion synthesis of silicon nitride. *Mater. Res. Bull.* **2008**, *43*, 1598–1606. [[CrossRef](#)]
26. Liu, G.; Chen, K.; Zhou, H.; Li, J.; Pereira, C.; Ferreira, J. Mechanical-activation-assisted combustion synthesis of  $\alpha$ -SiAlON in air. *Mater. Res. Bull.* **2007**, *42*, 989–995. [[CrossRef](#)]
27. Lapshin, O.; Ivanova, O. Macrokinetics of mechanochemical synthesis in heterogeneous systems: Mathematical model and evaluation of thermokinetic constants. *Mater. Today Commun.* **2021**, *28*, 102671. [[CrossRef](#)]
28. Smolyakov, V.K.; Lapshin, O.V.; Maksimov, Y.M. Macrokinetics of Mechanochemical Synthesis in Solid-Gas Systems. I. Mathematical Simulation. *Combust. Explos. Shock Waves* **2005**, *41*, 554–565. [[CrossRef](#)]

29. Smolyakov, V.K.; Itin, V.I.; Golobokov, N.N.; Kasatskii, N.G.; Lapshin, O.V.; Maksimov, Y.M.; Terekhova, O.G.; Shkoda, O.A. Macrokinetics of Mechanochemical Synthesis in Solid-Gas Systems. II. Experimental Studies. Analysis of Results. *Combust. Explos. Shock Waves* **2005**, *41*, 566–572. [[CrossRef](#)]
30. Córdoba, J.; Alcalá, M.; Avilés, M.; Sayagues, M.J.; Gotor, F. New production of TiC<sub>x</sub>N<sub>1-x</sub>-based cermets by one step mechanically induced self-sustaining reaction: Powder synthesis and pressureless sintering. *J. Eur. Ceram. Soc.* **2008**, *28*, 2085–2098. [[CrossRef](#)]
31. Calka, A.; Williams, J. Synthesis of Nitrides by Mechanical Alloying. *Mater. Sci. Forum* **1992**, *88–90*, 787–794. [[CrossRef](#)]
32. El-Eskandarany, M.S. Reactive Ball Milling to Fabricate Nanocrystalline Titanium Nitride Powders and Their Subsequent Consolidation Using SPS. *J. Mater. Eng. Perform.* **2017**, *26*, 2954–2962. [[CrossRef](#)]
33. El-Eskandarany, M.S.; Sumiyama, K.; Aoki, K.; Suzuki, K. Morphological and structural evolutions of nonequilibrium titanium-nitride alloy powders produced by reactive ball milling. *J. Mater. Res.* **1992**, *7*, 888–893. [[CrossRef](#)]
34. Oghenevweta, J.E.; Wexler, D.; Calka, A. Understanding reaction sequences and mechanisms during synthesis of nanocrystalline Ti<sub>2</sub>N and TiN via magnetically controlled ball milling of Ti in nitrogen. *J. Mater. Sci.* **2017**, *53*, 3064–3077. [[CrossRef](#)]
35. Shkoda, O.A.; Lapshin, O.V. Features of mechanochemical synthesis in the system of solid reagent—Active gas. *J. Phys. Conf. Ser.* **2018**, *1115*, 042014. [[CrossRef](#)]
36. Smolyakov, V.K.; Lapshin, O.V.; Maksimov, Y.M. Nonisothermal Interaction of Powders with a Reactive Gaseous Medium During Grinding. *Combust. Explos. Shock Waves* **2003**, *39*, 659–669. [[CrossRef](#)]
37. Gale, W.F.; Totemeier, T.C. (Eds.) *Smithells Metals Reference Book*, 8th ed.; Elsevier Inc.: Amsterdam, The Netherlands, 2004; 2072p.
38. Levashov, E.A.; Kurbatkina, V.V.; Rogachev, A.S.; Kochetov, N.A. Mechanoactivation of SHS systems and processes. *Int. J. Self-Propagating High-Temp. Synth.* **2007**, *16*, 46–50. [[CrossRef](#)]
39. Wriedt, H.A.; Murray, J.L. The N-Ti (Nitrogen-Titanium) system. *Bull. Alloy. Phase Diagr.* **1987**, *8*, 378–388. [[CrossRef](#)]